Article

Evaluation of Slope Stability in an Urban Area as a Basis for Territorial Planning: A Case Study

Paúl Carrión-Mero [1,2,*], Josué Briones-Bitar [1,2,*], Fernando Morante-Carballo [1,3,4], David Stay-Coello [5], Roberto Blanco-Torrens [6] and Edgar Berrezueta [7]

1   Centro de Investigación y Proyectos Aplicados a las Ciencias de la Tierra (CIPAT), Campus Gustavo Galindo Km 30.5 via Perimetral, ESPOL Polytechnic University, Guayaquil P.O. Box 09-01-5863, Ecuador; fmorante@espol.edu.ec

2   Facultad de Ingeniería en Ciencias de la Tierra (FICT), Campus Gustavo Galindo Km 30.5 via Perimetral, ESPOL Polytechnic University, Guayaquil P.O. Box 09-01-5863, Ecuador

3   Facultad de Ciencias Naturales y Matemáticas (FCNM), Campus Gustavo Galindo Km. 30.5 Vía Perimetral, ESPOL Polytechnic University, Guayaquil P.O.Box 09-01-5863, Ecuador

4   Geo-recursos y Aplicaciones GIGA, Campus Gustavo Galindo Km. 30.5 Vía Perimetral, ESPOL Polytechnic University, Guayaquil P.O. Box 09-01-5863, Ecuador

5   Facultad de Ciencias Matemáticas y Físicas, Universidad de Guayaquil, Cdla. Universitaria "Salvador Allende", Guayaquil 090514, Ecuador; david.stayc@ug.edu.ec

6   Facultad de Geología y Minas, Instituto Superior Minero Metalúrgico (ISMM), 83310 Moa, Cuba; rblanco@espol.edu.ec

7   Departamento de Infraestructura Geocientífica y Servicios, Instituto Geológico y Minero de España (IGME, CSIC), C/Matemático Pedrayes 25, 33005 Oviedo, Spain; e.berrezueta@igme.es

*   Correspondence: pcarrion@espol.edu.ec (P.C.-M.); briones@espol.edu.ec (J.B.-B.); Tel.: +593-984167430 (J.B.-B.)

Featured Application: The application of a methodology for evaluating susceptibility to landslides and landslides, based on the experience of several researchers, has allowed the generation of a susceptibility map. This susceptibility map presents a correlation with the geophysical data, drilling and pits, which validates the application of the methodology carried out. Also, it has provided a basis for security measures and territorial planning.

Abstract: Slope stability is determined by pre-conditioning and triggering factors. The evaluation of the stability by scientific criteria provides crucial input into land-use planning and development. This work aimed to evaluate the slope stability of "Las Cabras" hill (Duran, Ecuador) through geological and geotechnical analysis and a susceptibility assessment that allowed the definition of areas potentially susceptible to landslide and detachment for land planning recommendations. The methodology included (i) analysis of background information about the study area; (ii) fieldwork, sampling and laboratory tests; (iii) assessment of susceptibility to landslides and detachment through a theoretical–practical evaluation (using suggestions by various authors); (iv) a safety factor assessment employing the simplified Bishop method; and (v) analysis of the relationship between susceptibility and stability. Sixteen geomechanical stations were evaluated. Of these, seven stations are characterised as category III (medium susceptibility), six stations as category IV (high susceptibility) and three stations as category V (very high susceptibility). According to the susceptibility zoning map, 58.09% of the total area (36.36 Ha) is in the high to very high susceptibility category. The stability analysis based on 16 critical profiles shows that three of these profiles have safety factor values of less than one (0.86, 0.82 and 0.76, respectively), and two profiles have values close to one (1.02 and 1.00). The northern area is conditioned mainly by a vertical slope with an outcrop of fractured and weathered sandstones, thereby favouring rockfall. The landslide vulnerability in the case of the southern zone is principally conditioned by the fact that the slope and dip are parallel. The described characterisation and susceptibility analysis provide a basis for security measures and territorial planning.

Keywords: stability; susceptibility to detachment; susceptibility to sliding; simplified Bishop method; geomechanical characterisation

1. Introduction

A landslide is the movement of a mass of rock, debris or soil down a slope under the influence of gravity [1,2]. They are considered serious natural geological hazards in many areas of the world [3–5]. Specifically, landslides are the second most notable geological disasters identified by the United Nations Development Program [6]. In general, landslides are controlled by several pre-conditioning factors (e.g., morphology, lithology, structural environment, vegetation and land use) and are induced by different triggers (e.g., heavy rain, earthquakes, volcanic eruptions and marine storms) [7–11]. Furthermore, as development expands into unstable hillside areas under the pressures of increasing population and urbanisation, human activity, such as deforestation or excavation of slopes for roads and construction sites, becomes an essential trigger of landslides [12–15].

As the most common natural geological hazard in mountainous areas, landslides often cause significant economic loss and human casualties [16,17]. For this reason, the evaluation of these phenomena has been a primary scientific duty in order to establish the zoning of the analysed territory and to identify the main objects exposed to risk [18,19]. These undertakings have received increasing amounts of attention from the scientific community in recent decades [20–22]. Various qualitative, quantitative and empirical approaches have been proposed in the scientific literature to assess hazards and risks arising from landslides, rockfalls or slope instability [23–28].

One of the most often used methods is susceptibility mapping. The first landslide maps were prepared in the 1970s [29,30], and their elaboration still implies a certain degree of interpretation and correlations with various factors (e.g., topography, geomorphology, geotechnical properties and vegetation) [31–33]. Susceptibility maps provide valuable information for disaster mitigation work and land planning strategies [34]. This approach yields a more precise sustainability assessment that includes identifying high-vulnerability areas, risk analysis, security arrangements and stabilisation [35,36].

The area studied in this contribution is "Las Cabras" hill, Duran, in Southwest Ecuador. The hill has a small population with the necessary infrastructure (e.g., houses, roads and electrical network). Nowadays, there are 1540 houses, of which 88.38% (1361 houses) are inhabited. The access roads are in poor condition, making it difficult for waste collection vehicles and water tank trucks to enter. In recent years, signs of instability (e.g., deterioration, fracturing and minor wall instabilities) have been reported on the slopes of "Las Cabras" [37,38]. This potential instability of the terrain could cause severe mass movements over time, affecting the population.

Our work aimed to evaluate the slope stability of "Las Cabras" hill (Duran, Ecuador) through geological and geotechnical analysis and a susceptibility assessment that allowed the definition of areas potentially susceptible to landslide and detachment for land planning recommendations. A zoning map with the most unstable areas is intended to provide a basis for present and future territory planning.

2. Setting of "Las Cabras" Hill, Duran

Duran canton consists of three parishes (Eloy Alfaro, El Recreo and Divino Niño) and has an area of 59 km^2. This canton is part of the Province of Guayas in Ecuador. Duran is located 5 km from Guayaquil. Generally, it has a flat relief with a few isolated elevations, such as that of "Las Cabras" hill [39] (Figure 1a). "Las Cabras" hill has an area of 0.36 km^2 and an approximate height of 80 m. According to the Population and Housing Census in Ecuador (INEC, by its acronym in Spanish) [40], 11,868 people live in the area.

The climate is tropical (sub-humid), with temperatures ranging between 20 and 27 °C. According to the annual averages between 1985 and 2013 [41], precipitation can be between 800 and 1000 mm/year.
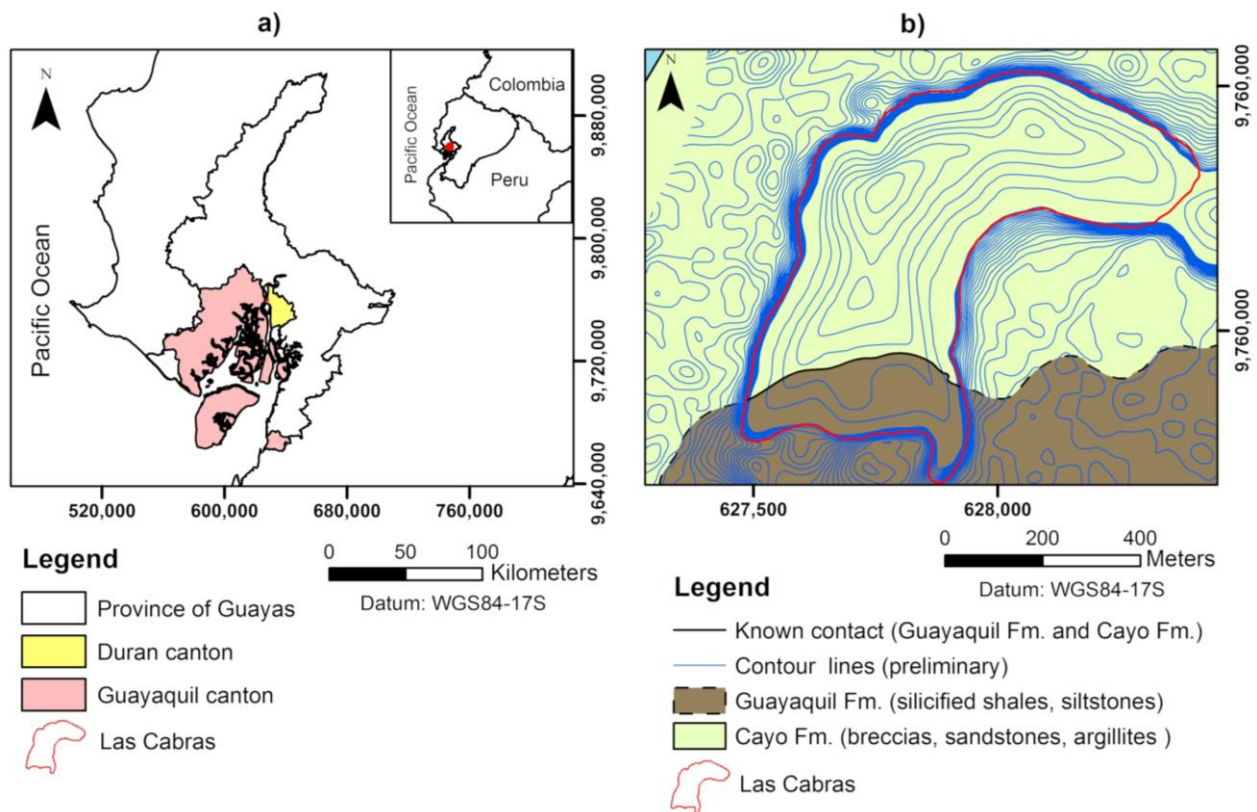
Figure 1. Location of the study area: (**a**) locations of Duran and Guayaquil cantons within the Province of Guayas, Ecuador; and (**b**) geology of the study area.

Water supply is delivered three days a week through pipes. The area has a local sewer system, but there is no description of its condition. The houses have septic tanks and latrines, and there is no official control over their operation. Rainwater circulates downstream through channels deepened parallel to the stairs on the slopes of the hill. Urban planning (construction of houses or essential services) is seriously lacking in the area.

The geology of the study area (Figure 1b) is represented mainly by the Cayo Formation (Upper Cretaceous), which consists of breccias, microbreccias, sandstones, shales even clays and argillites [42]. In general, these lithologies alternate and form centimetre to meter-thick bodies. The geological structure dips southwards with a slope of 15 to 25 degrees [43]. Significant colluvial soil development has taken place on top of the base rock, and some soils show signs of the current movement and instability (rotational rupture). A small part (in the southern part of the study area; see Figure 1b) corresponds to the Guayaquil Formation. Guayaquil Fm. consists of silicified shales and flint nodules that alternate with brown tubaceous siltstones [44] and sandstones with calcareous cement that belong to the Cayo Fm. [45].

3. Methodology

The methodology followed in this study (Figure 2) consisted of three phases: (i) analysis of background information about the study area; (ii) field survey and geological–geomechanical studies; and (iii) landslide susceptibility zoning.

3.1. First Phase

The first step was to compile relevant literature (articles, reports and press releases) related to the study area. Data provided by the project "Studies and proposals for the stabilisation of "Las Cabras" hill" were also collected [33]. This phase focused on developing the detailed topography of "Las Cabras" hill using GPS Satellite GNSS S82T equipment, and a SOKKIA SET 630 total station. An inventory was completed of the constructions in

the area (buildings, roads, water supply and septic tanks) to consider whether these could influence the terrain's instabilities. Finally, the technical and social context was analysed to consider the causes and impacts of the problem (instabilities).
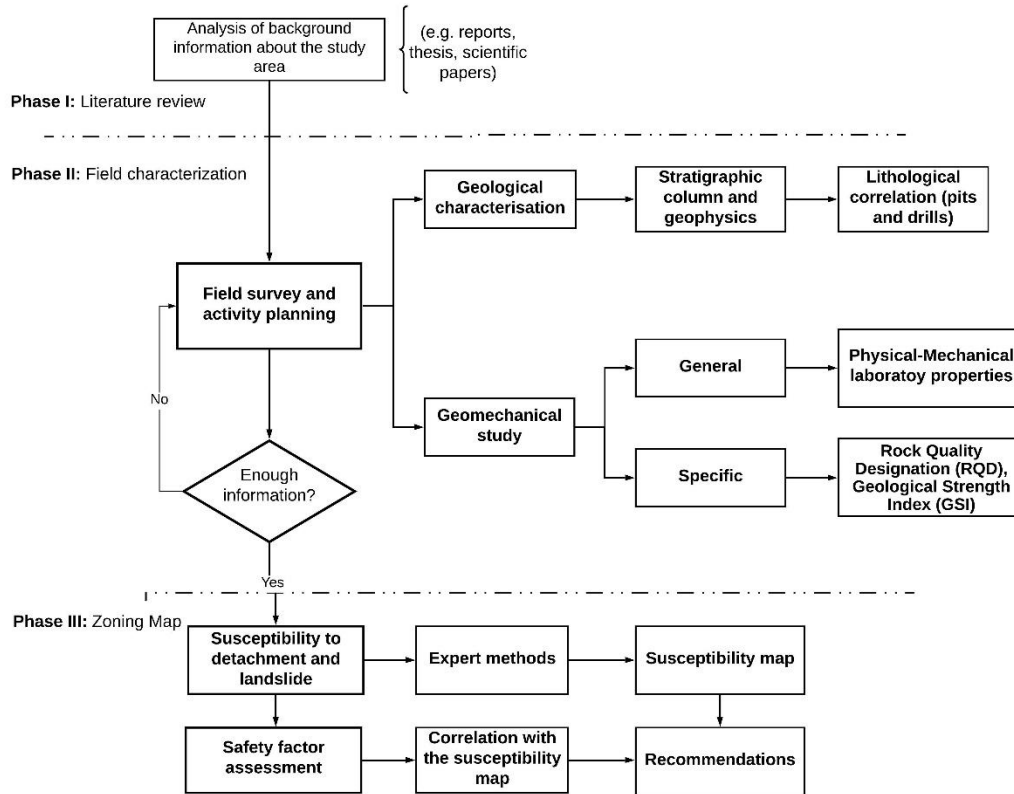

Figure 2. The proposed methodology for this study.

3.2. Second Phase

3.2.1. Geological Characterisation

The fieldwork at "Las Cabras" hill focused on studying the terrain's morphology and obtaining measurements of heading and dip of strata and other geological structures. Three geological sections were made in the study area, and a representative stratigraphic column.

Based on the identification of areas of geological interest, 18 vertical electrical soundings (VESs) were planned using the Schlumberger method [46,47]. The VESs carried out allowed estimating the thickness of the layers at depth. To verify the information obtained from the VESs, strategic points were established for drilling and pits.

Three rotational type boreholes were drilled with sample recovery. Six VESs close to the perforations were chosen to correlate them. Additionally, eight pits were made (excavations of at least one meter deep) to analyse in detail the materials (rocks and soils) present (see Figure 3). These actions allowed an adequate geological interpretation of the study area through the correlations of geoelectric profiles, the geological field survey and the geological drilling record.

3.2.2. General Geomechanical Study

The geomechanical study addressed the characterization of 16 stations (ordered set of geomechanical observations) in the study area (Figure 3). The number of stations and location depend on the favourable terrain conditions (existing outcrops and accessibility) and representativeness concerning their susceptibility to landslide or detachment (explained in Section 3.3). Eight geomechanical rock stations and eight soil stations were focused on in the study (Figure 4a,b). The number of stations studied was limited due to budget constraints, access permits and terrain.
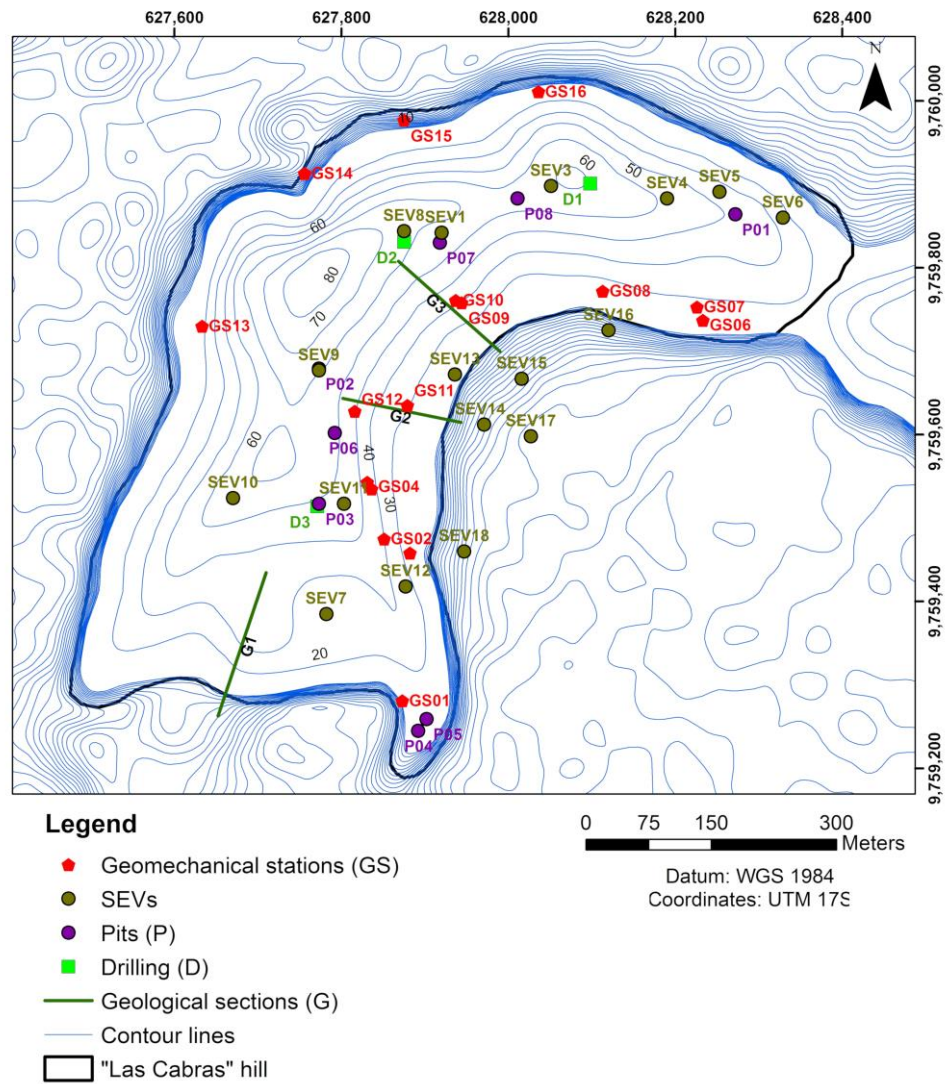
Figure 3. Locations of sites for geological and geomechanical characterisation studies.

(**a**)   (**b**)

Figure 4. (**a**) Sandstone rock mass with intercalations. (**b**) Lateritic soil product of residual shale weathering.

Eight rock samples were taken using the combo and chisel or easily removable blocks. Laboratory tests were carried out on each of the collected samples to evaluate their physical–mechanical properties. Simple linear compression, resistance, density, cohesion and angle of internal friction were tested on the samples. All tests were carried out in a specialised rock mechanics laboratory.

It is important to note that the linear compressive strength was determined by the "standard" method using cores with a height/diameter ratio of 1.5. The "Brazilian test" method was used for tensile strength. According to [48,49], the Brazilian test is a simple indirect test method to obtain the tensile strength of brittle material such as concrete, rock or rock-like material, in which a thin circular disk is diametrically compressed to failure. Cohesion and internal friction angle values were established using Mohr–Coulomb stress circles [50,51] from compressive and tensile strength values. To verify the results, we used former data obtained in the same area for other projects. These physical–mechanical properties were used for the determination of the stability conditions [21]

3.2.3. Specific Geomechanical Study

For this experimentation phase, the geomechanical rock stations, previously defined, were used for a specific analysis. A set of geomechanical parameters was used to characterise rock quality, such as the rock quality designation (RQD), the geological strength index (GSI), the degree of weathering and the lithostructural groups. These geomechanical parameters made it possible to characterise the conditions of landslide and detachment susceptibility that currently exist in "Las Cabras" hill.

Rock Quality Designation (RQD)

According to Deere [52], the RQD is a modified core recovery percentage, in which all pieces of sound core over 100 mm (4 in.) long are summed and divided by the length of the core run. The RQD index is an index of rock quality "in that problematic rock that is highly weathered, soft, fractures, sheared and jointed is counted against the rock mass" [52] (Table 1).

Table 1. RQD values according to Deere [52].

RQD%	Quality
<25	Very poor
25–50	Poor
50–75	Fair
75–90	Good
90–100	Excellent

For field observations, we applied the methodology given by Palmstrom [51] (Equation (1) and Table 2), where the RQD parameter is estimated using a correlation with the volumetric joint count (Jv).

$$J_v = \sum_{i=1}^{n} \frac{1}{S_i}, \tag{1}$$

where Si is the average spacing for the joint sets

Table 2. Correlation between RQD and volumetric discontinuity according to Palmstrom [53].

RQD%	Condition
RQD = 115–3.3 J_v	Si J_v > 4.5
RQD = 100	Si J_v ≤ i J

Weathering Degree, Geological Resistance Index (GSI) and Lithostructural Group

The study of the weathering degree, which implies reduced resistance, altered physical state and variation of the tension state on the slope or slopes, is necessary for the

engineering–geological evaluation [54–56]. The weathering degree was determined by visual observation and by the method proposed by Suárez [57], based on the International Society of Rock Mechanics (ISRM) reference value [53,58] (Table 3).

Table 3. Weathering degree based on ISMR [53].

Term	Description	Weathering Degree
Fresh	No visible sign of rock material weathering. Perhaps slight discolouration on major discontinuity surface.	I
Slightly weathered	Discolouration indicates weathering of rock material and discontinuity surfaces. All rock material may be discoloured by weathering.	II
Moderately weathered	Less than half of the rock material is decomposed or disintegrated into the soil. Fresh or discoloured rock is present either a a continuous framework or as a core stone.	III
Highly weathered	More than half of the rock material is decomposed or disintegrated into the soil. Fresh or discoloured rock is present either as a continuous framework or as a core stone.	IV
Completely weathered	All rock material is decomposed or disintegrated into the soil. The original mass structure is still largely intact.	V
Residual soil	All rock material is converted to the soil. The mass structure and the material fabric is destroyed. There is a significant volume change, but the soil has not been significantly transported.	VI

GSI is a system for characterizing the geomechanical properties of the rock mass through easy identification by visual evaluation of geological properties in the field [57]. The rock mass was characterised with the GSI using the table given by Hoek [59,60]. Finally, the different materials were classified according to the lithostructural groups established by Nicholson and Hencher [61]: strong massive rock (I), strong discontinuous rock (II), composite rock (III), tectonically weakened rock (IV), weak granular rock (V), karst rock (VI), anisotropic rock and ground-like rock (VII).

3.3. Third Phase

3.3.1. Detachment and Landslide Susceptibility

The theoretical–practical evaluation procedure used in this phase was based on the criteria of several authors, such as Ambalagán [62], Suárez [57], González, [63], Nicholson [61] and Blanco [33]. The geomechanical characteristics were defined (Tables 4 and 5) by assigning values attained following expert criteria. The selected parameters were lithology, geological structure, morphometry, discontinuity, water presence, vegetable cover, seismic activity and weathering rank, which were evaluated from 0 to 4 (Supplementary Table S1) based on the conditions observed in the field (see definitions of the parameters in Supplementary Table S2).

Table 4. Main parameters and weights assigned to rock mass in the susceptibility coefficient estimation, based on [21,57,61,63,64].

Parameter	Weight
Lithology (L)	0.0 to 4.0
Geological structure (Gs)	0.0 to 4.0
Morphometry (M)	0.0 to 4.0
Discontinuity (D)	0.0 to 4.0
Weathering rank (Wr)	0.0 to 4.0
Water presence (W)	0.0 to 3.0
Vegetable cover (Vc)	0.0 to 3.0
Seismic activity (S)	0.0 to 4.0
SC: (L + Gs + M + D + Wr + W + Vc + S)	0.0 to 30.0

Table 5. Main parameters and weights assigned to soil in the susceptibility coefficient estimation, based on [21,57,61,63,64].

Parameter	Weight
Soil characteristic (quality) (Sq)	0.0 to 4.0
Geological structure (Gs)	0.0 to 4.0
Morphometry (M)	0.0 to 4.0
Weathering rank (Wr)	0.0 to 4.0
Water presence (W)	0.0 to 3.0
Vegetable cover (Vc)	0.0 to 3.0
Seismic activity (S)	0.0 to 4.0
SC: (Sq + Gs + M + Wr + W + Vc + S)	0.0 to 26.0

This method allows the susceptibility levels to detachment and landslide (Tables 6 and 7) to be defined. The susceptibility level is a qualitative value (I to V), and it is related to the susceptibility coefficient (SC) estimated [21,64]. Thus, the grade and susceptibility levels for rocks are: I for $SC \leq 5.0$; II for $5.0 < SC \leq 10.0$; III for $10.0 < SC \leq 15.0$; IV for $15.0 < SC \leq 20.0$; and V for $SC > 20.0$. The grade or susceptibility levels for soils are: I for $SC \leq 5.0$; II for $5.0 < SC \leq 8.0$; III for $8.0 < SC \leq 12.0$; IV for $12.0 < SC \leq 16.0$; and V for $SC > 16.0$. As a result, the susceptibility map of instability (detachment and landslide) was prepared from the geomechanical evaluations obtained using the geostatistical kriging tool that allows the values to be interpolated.

Table 6. Detachment susceptibility classification (rock mass). Based on [21,57,61,63,64].

Susceptibility Level	Susceptibility Coefficient (SC)	Description
I	Very low susceptibility $SD \leq 5.0$	Stable conditions
II	Low susceptibility: $5.0 < SD \leq 10.0$	Stable conditions Monitoring recommended
III	Median susceptibility: $10.0 < SD \leq 15.0$	Predominantly stable conditions Systematic monitoring required
IV	High susceptibility: $15.0 < SD \leq 20.0$	Potentially unstable conditions
V	Very high susceptibility: $SD > 20.0$	Unstable conditions

Table 7. Landslide susceptibility classification (soil). Based on [21,57,61,63,64].

Susceptibility Level	Susceptibility Coefficient (SC)	Description
I	Very low susceptibility $SD < 5.0$	Stable conditions
II	Low susceptibility: $5.0 < SD \leq 8.0$	Stable conditions. Monitoring recommended
III	Median susceptibility: $8.0 < SD \leq 12.0$	Predominantly stable conditions Systematic monitoring required
IV	High susceptibility: $12.0 < SD \leq 16.0$	Potentially unstable conditions
V	Very high susceptibility: $SD > 16.0$	Unstable conditions

3.3.2. Safety Factor Assessment

Slope stability was assessed by the 2-dimensional stability program (SLIDE), which is based on the limit equilibrium calculation method [65]. Profiles were drawn according to the geomechanical stations and detailed topography. These were analysed in a static analysis (considering only the geotechnical characteristics of the terrain and the topography) and a pseudostatic analysis (considering the seismic activity of the study area).

We used seismic activity values established by the Ecuadorian Construction Standard (NEC-15, by its acronym in Spanish) [66]. According to [61], the study area is considered a zone of high seismic intensity, with a peak ground acceleration (seismic acceleration) of 0.40 g. However, in the pseudostatic analyses, 60% of the acceleration (i.e., 0.24 g) must be considered. Simplified Bishop methods were used to calculate the safety factor (SF). The simplified Bishop method uses the method of slices to discretise the soil mass and

determine the SF. This method satisfies the vertical force equilibrium for each slice and overall moment equilibrium about the centre of the circular trial surface. Since horizontal forces are not considered at each slice, the simplified Bishop method also assumes zero interslice shear forces [67,68]. The parameters input in the software SLIDE: the number of slices was 25 with a maximum number of iterations of 50. In this analysis, water table values were not considered.

Based on the susceptibility levels to detachment and landslide and the safety factor for rocks and soils, the obtained results were evaluated to establish the viability of the applied methodology.

4. Results

4.1. General Characterisation

Fieldwork on "Las Cabras" hill revealed inefficient development of essential services such as sanitary sewers, storm sewers, access roads and informal human settlements on surface watercourses. These could be considered instability triggers in the study area. The sanitary sewer system that fails to cover the needs of the entire population is of particular importance. Sixty percent of the houses were found to have septic tanks, and the other 40% had latrines. However, there is evidence of discharge escape towards the surface and infiltration into the ground in both cases.

The topographic work yielded a detailed, up-to-date topography of "Las Cabras" hill with UTM coordinates, which allowed us to draw the topographic plan of the study area (Figure 5b).
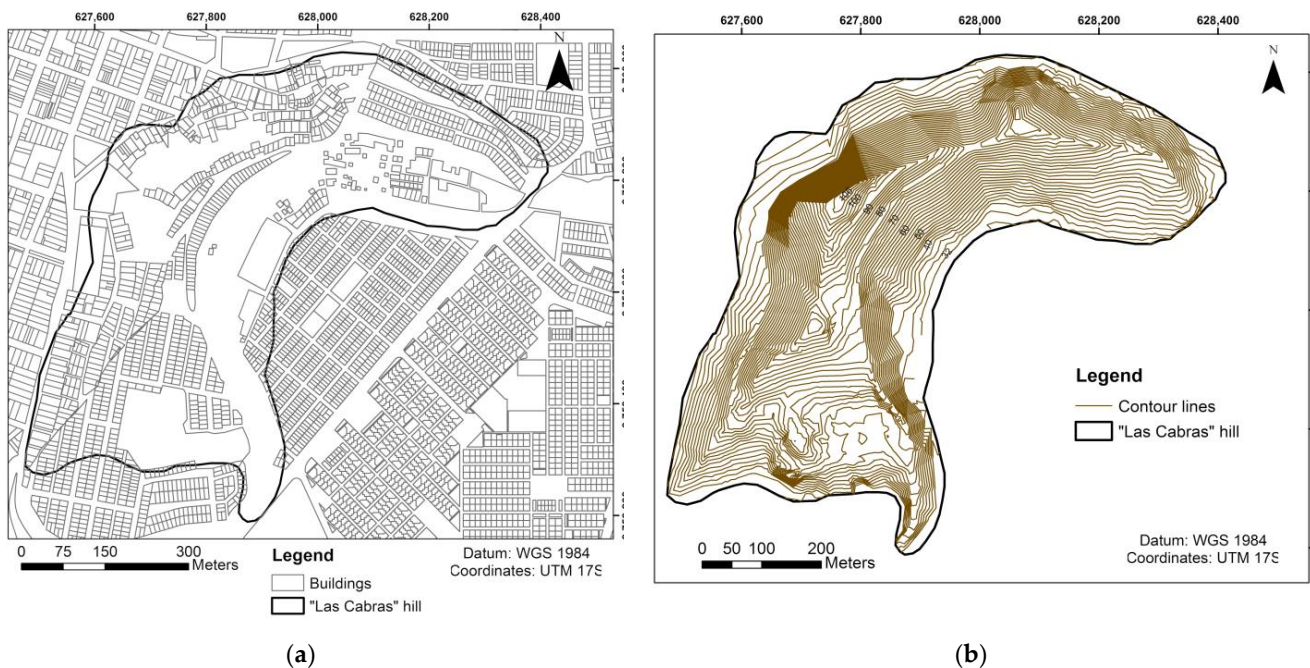

(**a**)

(**b**)

Figure 5. (**a**) Map of housing in the study area. (**b**) Detailed topography of the study area.

4.2. Geological Characterisation

4.2.1. Stratigraphy

The field data obtained show a sedimentary succession that consists of metric brecciated and microbrechified bodies formed by angular ridges of sizes ranging from centimetric to decimetric. It has a shale composition. Glauconite is present, as are mafic volcanic fragments and medium and fine-grained sandstones. The shale interval is characterized by the presence of intercalations of those medium and fine-grained sandstones. We also saw in the shales parallel laminations and normal and inverse gradations. Subsequently, and with net contact, a succession of centimetre and decimetric layers of medium-grained

sandstones, siliceous chert shales and fissile shales are present. This layer is overlaid by a set of unconsolidated colluvium/breccia with intercalations of medium-grained sandstones and shales. Colluvial material appears on the top of the sedimentary succession (Figure 6).
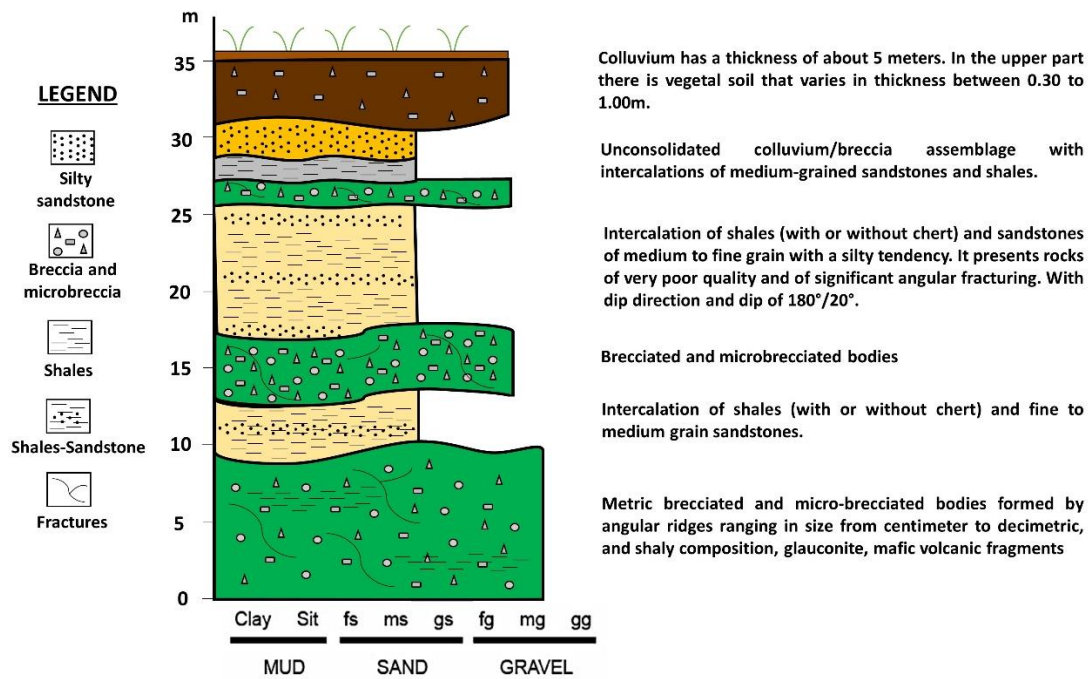

Figure 6. Slope stratigraphic column.

The lithological layers have a preferential dip of 15–20° and a dip direction of 180–200°. The studied area is strongly fractured (three families of discontinuities: 180°/22°, 170°/16° and 140°/53°). Raised lithological units reached a thickness of 35 m. This data are complemented by the geological profiles made that are presented in Supplementary Figures S1–S3 and Supplementary Table S3.

4.2.2. VESs

Eighteen VESs have been interpreted with IPI2win software (versión 3.0.1), and resistivity curves were adjusted to represent the strata with an error of less than 6%. Table 8 shows the lithologies based on the resistivities determined in the VESs. The interpretations of the 18 VESs can be seen in Supplementary Table S4.

Table 8. Geoelectrical interpretation of the lithology based on VESs.

| Interpretation	Resistivity (Ωm)
Colluvium-Anthropic Fill	0.0–20.0
Shales	20.0–45.0
Fractured silty sandstone	45.0–100.0
Compact sandstone	100.0–600.0
Breccia/microbreccia	>600.0

4.2.3. Pits

In the geological studies carried out in the pits, stratigraphic columns were constructed (an example is seen in Table 9).

In Table 9 (representative of the eight pits), we can see that the column reaches a depth of 2.50 m. In general, the levels determined in this section correspond to (from base to top): sandstones and microbreccias with glauconite, medium-grained sandstones, medium-

grained sandstones and dark shales and soil. Information from all pits is presented in Supplementary Table S5.

Table 9. Stratigraphic column of pit P08.

Coordinates: 628011/9759883
Depth: approximately 2.50 m
Description: Pit in possible artificial fill over sandy-clay soil with sandstones, shales and microbreccias.
Vegetable earth: Humus with abundant roots with a thickness of 25 cm. Centimetre to decimetre sized clasts of dark shales and sandstones.
Water level: Not apparent
Detailed description:
0.00–0.25 m: humus with abundant roots and some centimetric-decimetric clasts of dark shales and sandstones. Matrix-supported texture.
0.25–1.00 m: predominance of decimetre size clasts in sandy-clay matrix (grain-supported texture). The clasts are medium-grained sandstones and dark shales.
1.00–1.60 m: medium-grained sandstones, presenting typical concentric fractures, along which fine-grained sandstones appear.
1.60–2.50 m: microbreccias with glauconite.
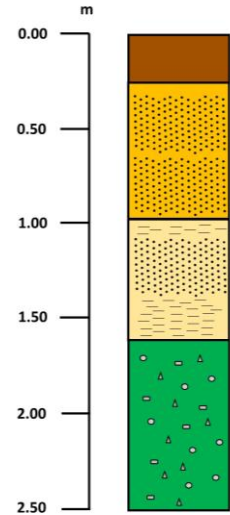
4.2.4. Drilling

Table 10 shows the lithologies based on the samples recovered from the boreholes and the depths reached in each one. The materials obtained from the drilling are mainly sandstones and shales from the Cayo Formation. A more detailed description of each drilling can be seen in Supplementary Table S6.

Table 10. Information of boreholes.

Drill	D1	D2	D3
Coordinates	628098/9759901	627875/9759831	627771/9759514
Rock mass	Sandstones	Clay soil, shales and sandstones.	Sandstones and shales.
Depth (m)	7.00	6.00	5.00

4.2.5. VESs and Drilling Correlation

Three correlations have been made between VESs and perforations using kriging interpolation. One of the correlations between drilling D1 and the VESs close to it (VES3 and VES4) is presented in Figure 7. Two other correlations have been made with drilling D2 with VES1 and VES8 and drilling D3 with VES10 and VES11. These can be seen in Supplementary Figures S4 and S5.

4.3. Geomechanical Study

4.3.1. Description of Materials and Physical-Mechanical Properties

The materials defined from pits and outcrop characterisation are generally sandstones and shales from the Cayo Fm. The data in the columns can be extrapolated to the geomechanical stations. Of the 16 geomechanical stations defined, results of the physical–mechanical characterization of rocks were obtained. Table 11 demonstrates that sandstone is the most common rock type, according to the characteristic of the Cayo Fm. The rock samples were of fair quality (270–685 Kg/cm^2).
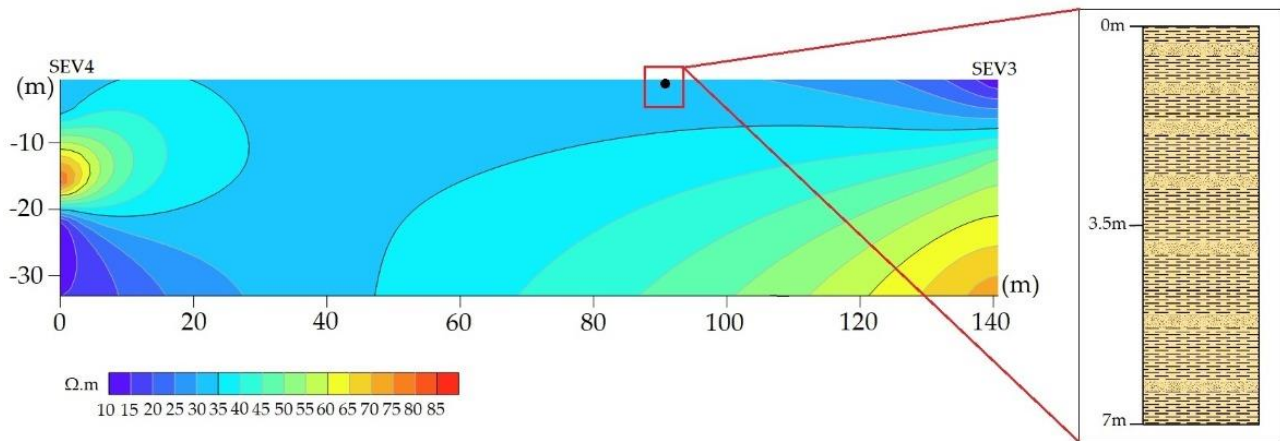
Figure 7. Correlations between the VESs (4-3) and drilling D1. It can be seen that the material obtained from drilling D1 (shales) coincides with the resistivity presented (values between 35.0 and 40.0).

Table 11. Physical–mechanical properties of rock samples from geomechanical stations.

Station	Rock Type and Characteristics	Density (g/cm³)	Compressive Strength (Kg/cm²)	Cohesion (Kg/cm²)	Friction Angle (Degrees)
GS02	Medium-grained sandstone	2.40	575	130	34–40
GS04	Siliceous shale	2.35	320	105	39–43
GS08	Medium-grained sandstone	2.50	605	140	40–43
GS10	Fine-grained sandstone	2.38	410	110	34–38
GS13	Medium-grained sandstone	2.54	685	150	36–43
GS14	Sandstone with intercalations of high compressive strength rocks	2.62	655	125	37–42
GS15	Medium-grained sandstone	2.40	475	120	32–38
GS16	Sandstone with intercalations of low compressive strength rocks	2.35	270	115	37–41

4.3.2. Geomechanical Characteristics of Soil and Rock Stations

The results of the geomechanical characterisation of rock stations are shown in Table 10. The study in the geomechanical soil stations revealed a moderate to residual weathered soil degree. Additionally, these stations are characterized by no water to minimal surface water, and from little vegetation to being largely covered by adequate vegetation. In the case of the characterised soils, it was found that the predominant soil is represented by clayey colluvial soil, with weathered sandstone blocks of medium grain (Table 12).

Table 12. Description of geomechanical soil stations.

Station	Soil Description (Characteristic)	Geological Structure	Water Presence	Vegetable Cover	Weathering Degree
GS01	Residual soil formed by shale weathering	Weakness planes favour sliding	No water presence	Little vegetation cover	Residual soil
GS03	Predominantly sandy-wet soil, significant clayey fraction	Slope position somewhat favourable concerning weakening planes	Minimal surface waters action	No vegetation cover	Moderately weathered

Table 12. *Cont.*

Station	Soil Description (Characteristic)	Geological Structure	Water Presence	Vegetable Cover	Weathering Degree
GS05	Predominantly clayey colluvial soil, with weathered sandstone blocks of medium grain	Slope position somewhat favourable concerning weakening planes	No water presence	Covered mainly by adequate vegetation cover	Moderately weathered
GS06	Colluvium of clay composition and plastic behaviour	Slope position somewhat favourable concerning weakening planes	No water presence	Covered mainly by adequate vegetation cover	Slightly weathered
GS07	Predominantly clayey soil with a high level of humidity and plastic behaviour	Weakness planes favour sliding	No water presence	Partially covered by adequate vegetation cover	Slightly weathered
GS09	Soil consisting of little compacted plastic clays	Slope position somewhat favourable concerning weakening planes	Minimal surface waters action	Covered mainly by adequate vegetation cover	Moderately weathered
GS11	Very dry, compact clay with a high sand fraction	Weakness planes favour sliding	Minimal surface waters action	No vegetation cover	Completely weathered
GS12	Alluvium	Weakness planes favour sliding	Minimal surface waters action	No vegetation cover	Completely weathered

The results of the geomechanical characterisation of rock stations are shown in Table 13. The weathering degree values are in categories II and III, and the GSI values are between 70 and 60. The RQD values are between 55 and 70%. Lithostructural group values are in categories II and III.

Table 13. Geomechanical characteristics of the rock stations.

Station	RQD (%)	WeatheringRank	GSI	Lithostructural Group	Vegetal Cover	Discontinuity
GS02	55–65	IV	70–60	III	No vegetation cover	600 mm spacing, aperture 0.5 mm
GS04	50–60	III	70–60	II	Covered mainly by adequate vegetation cover	150 mm spacing, aperture between 3.0 and 4.0 mm
GS08	50–60	III	70–60	II–III	Covered mainly by adequate vegetation cover	600 mm spacing, aperture between 0.6 and 0.8 mm
GS10	55–70	III	70–60	II–III	Little vegetation cover	200 to 600 mm spacing, aperture between 0.5 and 1.0 mm
GS13	55–65	III	70–60	II–III	Partially covered by adequate vegetation cover	600 mm spacing, aperture 0.5 mm
GS14	55–70	III	65–50	II	Partially covered by adequate vegetation cover	400 to 500 mm spacing, aperture between 0.7 and 1.0 mm
GS15	55–70	III	65–50	II	Partially covered by adequate vegetation cover	200 to 600 mm spacing, aperture between 0.5 and 1.0 mm
GS16	50–60	III	70–60	II	Partially covered by adequate vegetation cover	600 mm spacing, aperture 1.0 mm

4.4. Detachment and Landslide Susceptibility

According to the proposed susceptibility classifications, Tables 14 and 15 present the overall mass movement susceptibility assessment (Tables 6 and 7). Figure 8 shows the zoning of the study area.

Table 14. Assessment of landslide susceptibility in soils.

Susceptibility Category	Stations in Soil							
	GS01	GS03	GS05	GS06	GS07	GS09	GS11	GS12
III			12.0	11.5	12.5	11.5		
IV		15.5						
V	19.5						20.0	19.5

Table 15. Assessment of detachment susceptibility in rock mass.

Susceptibility Category	Stations in Rock							
	GS02	GS04	GS08	GS10	GS13	GS14	GS15	GS16
III		15.0	15.00	15.0				
IV	16.0				17.5	17.5	17.5	17.5
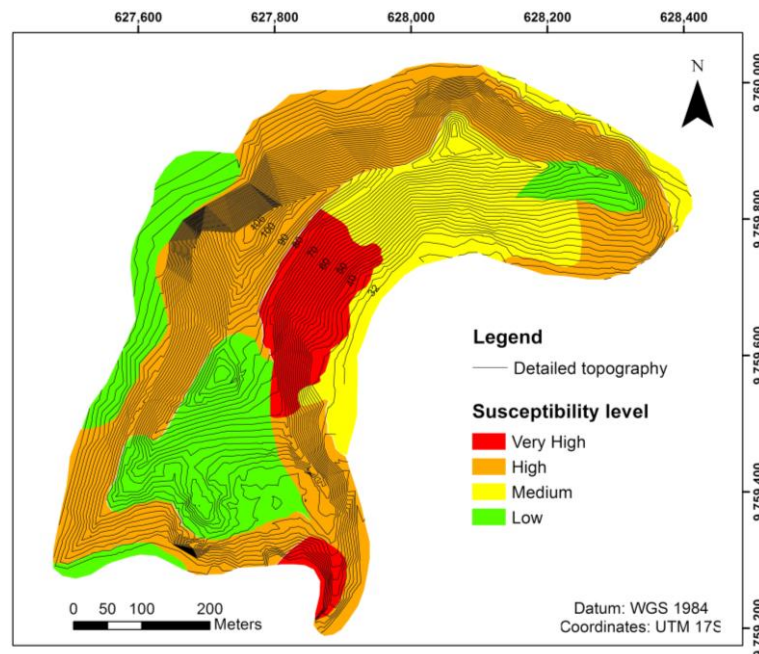
Figure 8. Zoning plan according to susceptibility to landslide and detachment.

In soils (Table 12), four stations (GS05–GS07, GS09) were found to belong to landslide susceptibility category III, one (GS03) to category IV and three (GS01, GS11 and GS12) to category V. In rocks (Table 13), three stations (GS04, GS08, GS10) fall into category III, and five stations (GS02, GS13–GS16) into category IV. Regarding the areas in Figure 7, 22.80% of the total area has low susceptibility, 19.11% medium susceptibility, 48.54% high susceptibility and 9.55% very high susceptibility.

4.5. Stability Assessment

The 16 critical profiles can be seen in Figure 9.
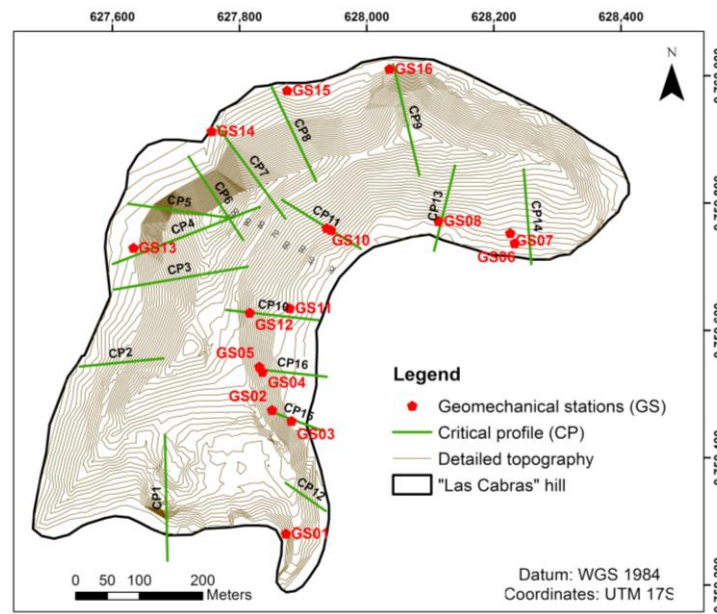
Figure 9. Critical profiles for stability assessment.

Figure 10a,b shows examples of profiles (CP12, Figure 9) in the SLIDE program in static and pseudostatic conditions. For the stability assessment, the geotechnical parameters of Table 16 were used, which were obtained from the results of Table 11. In some profiles, colluvium's presence was taken into account—its values of density, cohesion and friction angle present in a previous work were used [33].

Table 17 shows the comparison of the susceptibility analysis and the safety factors (SF) of the stability analysis in the SLIDE program (obtained from critical profiles in Figure 5). The safety factor was found to be between 0.76 and 2.64. Regarding susceptibility levels, the profiles CP10–CP16 range from high to very high susceptibility, while the profiles CP01–CP09 range from low to high.

(**a**)

Figure 10. *Cont.*

(b)
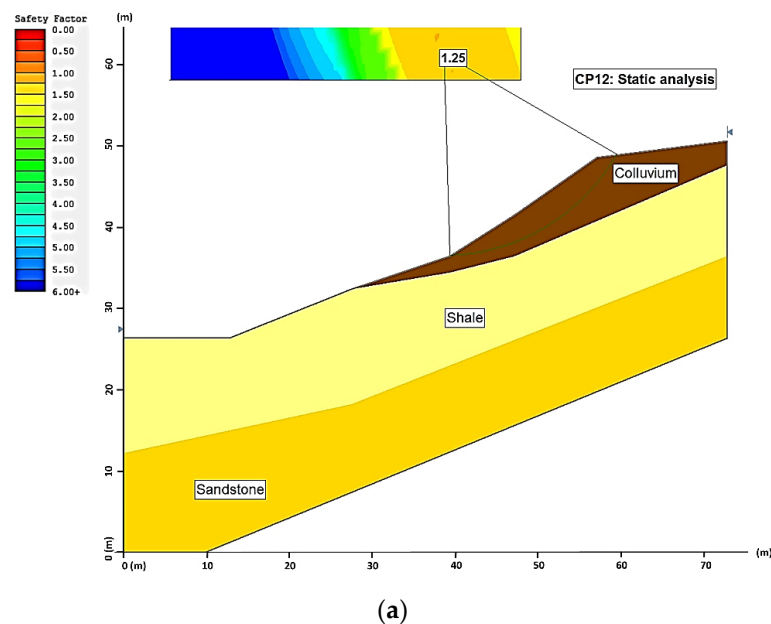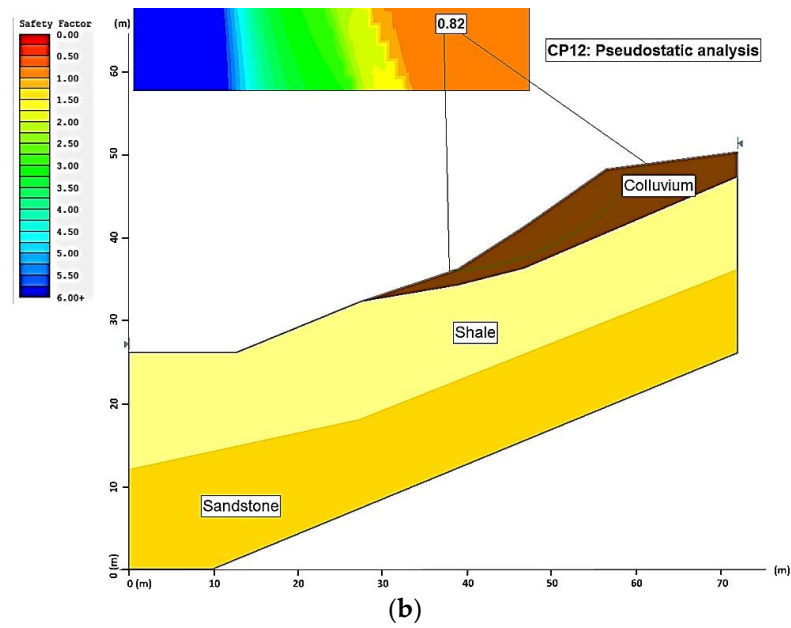
Figure 10. CP12 profile results in (**a**) static condition and (**b**) pseudostatic condition.

Table 16. Geotechnical parameters used in stability analysis. Colluvium data from [33].

Material	Density (kN/m^3)	Cohesion (kPa)	Friction Angle (Degrees)
Colluvium	21.00	10.00	25.00
Shale	26.00	14.00	42.00
Sandstone	28.00	20.00	38.00

Table 17. Results obtained from the stability analysis considering the 16 critical profiles.

Critical Profile	Susceptibility Coefficient (SC)	Static Condition (SF$_{static}$)	Pseudostatic Condition a$_s$ = 0.24 g (SF$_{pseudostatic}$)
CP01	Low to high	2.19	1.71
CP02	Low to high	3.66	2.64
CP03	Low to high	1.62	1.25
CP04	High	1.36	1.25
CP05	High	1.42	1.12
CP06	High	1.59	1.21
CP07	High	2.26	1.64
CP08	Medium to high	2.85	2.14
CP09	Medium to high	2.15	1.59
CP10	Very high	1.15	0.76
CP11	Medium to very high	2.07	1.16
CP12	High	1.25	0.82
CP13	Medium	1.51	0.88
CP14	High	2.43	1.26
CP15	High	1.48	1.00
CP16	Medium to high	1.69	1.02

5. Analysis of Results and Discussion

The sedimentary succession of "Las Cabras" hill (Duran) is characterised by the alternation of breccias, strongly fractured and weathered fine-grained silty sandstones, shales and argillites. The rock mass has a high weathering degree and both mechanical and chemical deterioration, which favours the formation of clay and residual soils. The instability observed on different slopes of "Las Cabras" hill is due to—among other causes—the dipping of the layers in the direction of the slope. This means that they are susceptible to different types of mass movement, as indicated by several authors [3,4].

Susceptibility was assessed (Figure 7) through a combination of methods, in which several geomechanical parameters were considered [21,57,61,63,64]. This allowed a specific categorisation (low to very high) of the landslide and rockfall conditions in the study area. The stability analysis demonstrated that different zones present an unstable equilibrium. Three of the studied profiles obtained values lower than one (profiles CP10, CP12 and CP13), and two profiles obtained values close to one (profiles CP15 and CP16). According to the NEC-15 [66], Melentijevic [69] and Morante et al. [21], safety factors (SF) less than one represent instability.

The zones classified with high and very high susceptibility (Figure 8) correspond to layers of shales and fractured sandstones. These zones were validated with the low resistivities (between 0 and 45 Ωm) in the first 15 m of the VESs carried out (Supplementary Table S4). Additionally, from the results of Table 15 (comparing SC and $SF_{pseudostatic}$), it can be observed that they agree with one another well. For example, the CP10 profile has a very high SC that agrees with the obtained SF of 0.76. Additionally, the CP04 profile has a high SC and agrees with the SF obtained of 1.25 (in Supplementary Figure S6 can be seen the zoning map using the safety factor). Thanks to these comparisons, the reliability of the applied expert methodology can be established. This methodology considers the experience of the researchers and the geological-geotechnical characteristics, the relief and the environmental characteristics of the study site. This method has been used to assess landslide and detachment susceptibility in areas of sub-vertical and vertical slopes, and urban areas or sites of direct or indirect impact on populations or heritage sites. [21,54,56,64].

The obtained results provide a basis for stabilisation measures, solutions and territorial planning that guarantee safety. As a guideline of territorial planning, if it is not possible to ensure security in a given area, it must be reorganised. Figure 11 indicates the areas that must be given top priority. Two zones were identified where human settlements are present and the landslide susceptibility is very high: area 1 (2.93 Ha) and area 2 (0.54 Ha).
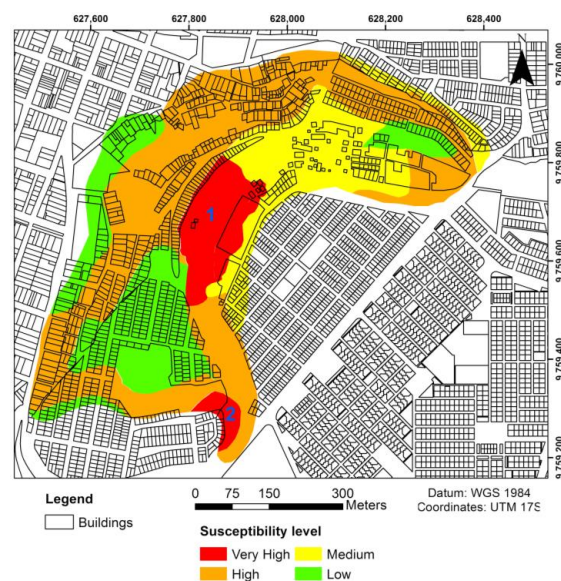

Figure 11. Housing and susceptibility zoning.

The stabilising measures should be selected so that they also generate added value. These works must start on the crown of the slope and proceed downwards. We do not propose to vacate houses, except those few that are particularly unsafe and are removed from the rest of the buildings. Solutions are proposed for both the southern and northern sides of "Las Cabras" hill. For the northern side, injected anchors (using gunite and Ø25 mm rods) and mechanical drains are proposed to reduce the water table in that area, and to be applied in combination with stairway-like surface channels to evacuate rainwater (Figure 12).
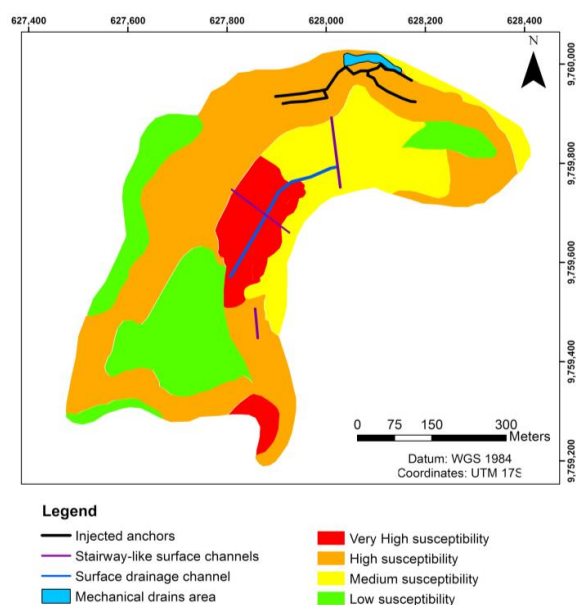
Figure 12. Recommended stabilization solutions by location in the study area.

Although a detailed study of triggers is beyond the scope of this study, a general approach is presented. Three possible factors were identified. Seismic activity is significant in the study area (up to 0.24 g [66]) and is considered a possible triggering factor. Furthermore, two anthropic factors, namely, the presence of houses in inappropriate places (without territorial planning) and a sewer system in poor condition, must also be considered as potential triggers. These anthropic factors were not considered in the current stability analysis.

In summary, the problematic situation in Las Cabras hill is mainly due to the instability characteristics of the rock mass (deterioration, fracturing and in some cases the dipping of the layers) and the action of anthropic effects. This situation is conditioned by:

- Instability of some slopes, due to, among other causes, the dip of the layers in the direction of the slope, the degree of fracturing and deterioration of the topmost ground layers. This facilitates erosion due to water flow through fissures, with the consequent destabilisation of the ground and buildings.
- The terrain's morphology, inadequate location and technical deficiencies of some of the constructions. Additionally, most buildings were constructed without any design or planning, which resulted in a chaotic distribution.
- Malfunction of the natural drainage system, which is clogged due to uncontrolled constructions. The lack of additional water drainage channels.

6. Conclusions

The diagnosis of the current situation regarding the stability of "Las Cabras" hill was established through a geological–geomechanical study that included evaluating stability and susceptibility to landslide and detachment and the calculation of safety factor. The obtained results revealed a slope, on the northwest side, of very high to high susceptibility to landslide and detachment (more than 60% of the total area) and unstable areas (with

SF less than 1). On the other hand, the most critical areas were the profiles CP10 to CP16 because the dip of the layers has a general south–southwest trend, which coincides with the slope of the terrain. It is recommended in critical sectors to leave buffer strips at the foot of these sectors and implement monitoring and protection measures.

As that part of the hill consists of competent and moderately competent rocks, three factors were considered to affect the possibility of mass movement: (a) problems with drainage (both rainwater and sewage); (b) negative anthropic actions (e.g., housing in inappropriate places, with direct and indirect consequences); and (c) the existing fracturing and weathering degrees of the rock.

Possible solutions to compensate for instabilities are based on controlling erosive processes on the rock masses that could move or slide. Solutions are proposed for both the north and south sides, including the implementation of injected anchors, mechanical drains and stairway-type surface channels to evacuate rainwater. These measures necessarily depend on territorial regulation and require constant monitoring due to the presence of buildings in the affected areas.

References

1. Cruden, D.M. A simple definition of a landslide. *Bull. Int. Assoc. Eng. Geol.—Bull. L'Association Int. Géologie l'Ingénieur* **1991**, *43*, 27–29. [CrossRef]
2. Gudiyangada Nachappa, T.; Tavakkoli Piralilou, S.; Ghorbanzadeh, O.; Shahabi, H.; Blaschke, T. Landslide Susceptibility Mapping for Austria Using Geons and with the Dempster-Shafer Theory. *Appl. Sci.* **2019**, *9*, 5393. [CrossRef]
3. Cruden, D.M.; Varnes, D.J. Landslide types and processes. *Spec. Rep. Natl. Res. Counc. Transp. Res. Board* **1996**, *247*, 36–75.
4. Fell, R.; Corominas, J.; Bonnard, C.; Cascini, L.; Leroi, E.; Savage, W.Z. Guidelines for landslide susceptibility, hazard and risk zoning for land use planning. *Eng. Geol.* **2008**, *102*, 85–98. [CrossRef]
5. Guzzetti, F.; Mondini, A.C.; Cardinali, M.; Fiorucci, F.; Santangelo, M.; Chang, K.T. Landslide inventory maps: New tools for an old problem. *Earth-Sci. Rev.* **2012**, *112*, 42–66. [CrossRef]
6. Azarafza, M.; Ghazifard, A.; Akgün, H.; Asghari-Kaljahi, E. Landslide susceptibility assessment of South Pars Special Zone, southwest Iran. *Environ. Earth Sci.* **2018**, *77*, 805. [CrossRef]
7. Segoni, S.; Rosi, A.; Rossi, G.; Catani, F.; Casagli, N. Analysing the relationship between rainfalls and landslides to define a mosaic of triggering thresholds for regional-scale warning systems. *Nat. Hazards Earth Syst. Sci.* **2014**, *14*, 2637–2648. [CrossRef]
8. Carrara, A.; Crosta, G.; Frattini, P. Geomorphological and historical data in assessing landslide hazard. *Earth Surf. Process. Landforms* **2003**, *28*, 1125–1142. [CrossRef]
9. Glade, T.; Crozier, M.J. Landslide geomorphology in a changing environment. *Geomorphology* **2010**, *120*, 1–2. [CrossRef]
10. Calista, M.; Miccadei, E.; Piacentini, T.; Sciarra, N. Morphostructural, meteorological and seismic factors controlling landslides in weak rocks: The case studies of Castelnuovo and Ponzano (north east Abruzzo, central Italy). *Geoscience* **2019**, *9*, 122. [CrossRef]
11. Dai, Z.; Guo, J.; Luo, H.; Li, J.; Chen, S. Strength Characteristics and Slope Stability Analysis of Expansive Soil with Filled Fissures. *Appl. Sci.* **2020**, *10*, 4616. [CrossRef]
12. Dai, F.C.; Lee, C.F.; Ngai, Y.Y. Landslide risk assessment and management: An overview. *Eng. Geol.* **2002**, *64*, 65–87. [CrossRef]
13. Gardner, J.S.; Dekens, J. Mountain hazards and the resilience of social-ecological systems: Lessons learned in India and Canada. *Nat. Hazards* **2007**, *41*, 317–336. [CrossRef]
14. Turconi, L.; Luino, F.; Gussoni, M.; Faccini, F.; Giardino, M.; Casazza, M. Intrinsic environmental vulnerability as shallow landslide susceptibility in environmental impact assessment. *Sustainability* **2019**, *11*, 6285. [CrossRef]
15. Mavroulis, S.; Triantafyllou, I.; Karavias, A.; Gogou, M.; Katsetsiadou, K.-N.; Lekkas, E.; Papadopoulos, G.A.; Parcharidis, I. Primary and Secondary Environmental Effects Triggered by the 30 October 2020, Mw = 7.0, Samos (Eastern Aegean Sea, Greece) Earthquake Based on Post-Event Field Surveys and InSAR Analysis. *Appl. Sci.* **2021**, *11*, 3281. [CrossRef]
16. Liu, S.; Segoni, S.; Raspini, F.; Yin, K.; Zhou, C.; Zhang, Y.; Casagli, N. Satellite InSAR as a New Tool for the Verification of Landslide Engineering Remedial Works at the Regional Scale: A Case Study in the Three Gorges Resevoir Area, China. *Appl. Sci.* **2020**, *10*, 6435. [CrossRef]
17. Froude, M.J.; Petley, D.N. Global fatal landslide occurrence from 2004 to 2016. *Nat. Hazards Earth Syst. Sci.* **2018**, *18*, 2161–2181. [CrossRef]
18. Mineo, S.; Pappalardo, G.; Mangiameli, M.; Campolo, S.; Mussumeci, G. Rockfall analysis for preliminary hazard assessment of the cliff of taormina Saracen Castle (Sicily). *Sustainability* **2018**, *10*, 417. [CrossRef]
19. Carrión Mero, P.; Blanco Torrens, R.; Borja Bernal, C.; Aguilar Aguilar, M.; Morante Carballo, F.; Briones Bitar, J. Geomechanical and Analysis of the Effects of Rock Massif in Zaruma City, Ecuador. In Proceedings of the LACCEI International Multi-Conference for Engineering, Education and Technology, Montego Bay, Jamaica, 24–26 July 2019; Latin American and Caribbean Consortium of Engineering Institutions: Boca Raton, FL, USA, 2019; Volume 2019.
20. Gordo, C.; Zêzere, J.L.; Marques, R. Landslide susceptibility assessment at the basin scale for rainfall- and earthquake-triggered shallow slides. *Geosciences* **2019**, *9*, 268. [CrossRef]
21. Morante, F.; Aguilar, M.; Ramírez, G.; Blanco, R.; Carrión, P.; Briones, J.; Berrezueta, E. Evaluation of Slope Stability Considering the Preservation of the General Patrimonial Cemetery of Guayaquil, Ecuador. *Geosciences* **2019**, *9*, 103. [CrossRef]
22. Sestraş, P.; Bilaşco, Ş.; Roşca, S.; Naş, S.; Bondrea, M.; Gâlgău, R.; Vereş, I.; Sălăgean, T.; Spalević, V.; Cîmpeanu, S. Landslides Susceptibility Assessment Based on GIS Statistical Bivariate Analysis in the Hills Surrounding a Metropolitan Area. *Sustainability* **2019**, *11*, 1362. [CrossRef]
23. Evans, S.G.; Hungr, O. The assessment of rockfall hazard at the base of talus slopes. *Can. Geotech. J.* **1993**, *30*, 620–636. [CrossRef]
24. Crosta, G.B.; Agliardi, F. A methodology for physically based rockfall hazard assessment. *Nat. Hazards Earth Syst. Sci.* **2003**, *3*, 407–422. [CrossRef]
25. Macciotta, R.; Martin, C.D.; Morgenstern, N.R.; Cruden, D.M. Quantitative risk assessment of slope hazards along a section of railway in the Canadian Cordillera—A methodology considering the uncertainty in the results. *Landslides* **2016**, *13*, 115–127. [CrossRef]
26. Barrantes Castillo, G.; Barrantes Sotela, O.; Núñez Roman, O. Efectividad de la metodología Mora-Vahrson modificada en el caso de los deslizamientos provocados por el terremoto de Cinchona, Costa Rica. *Rev. Geográfica América Cent.* **2011**, *2*, 141–162.
27. Anbalagan, R.; Chakraborty, D.; Kohli, A. Landslide hazard zonation (LHZ) mapping on meso-scale for systematic town planning in mountainous terrain. *J. Sci. Ind. Res.* **2008**, *67*, 486–497.
28. Briones-Bitar, J.; Carrión-Mero, P.; Montalván-Burbano, N.; Morante-Carballo, F. Rockfall Research: A Bibliometric Analysis and Future Trends. *Geosciences* **2020**, *10*, 403. [CrossRef]

29. Brabb, E.E.; Pampeyan, E.H.; Bonilla, M.G. Landslide susceptibility in San Mateo County, California. In *Miscellaneous Field Studies Map*; U.S. Geological Survey: Reston, CA, USA, 1972; Volume 360.

30. Kienholz, H. Maps of Geomorphology and Natural Hazards of Grindelwald, Switzerland: Scale 1:10,000. *Arct. Alp. Res.* **1978**, *10*, 168. [CrossRef]

31. Fell, R. Landslide risk assessment and acceptable risk. *Can. Geotech. J.* **1994**, *31*, 261–272. [CrossRef]

32. Rossi, M.; Guzzetti, F.; Reichenbach, P.; Mondini, A.C.; Peruccacci, S. Optimal landslide susceptibility zonation based on multiple forecasts. *Geomorphology* **2010**, *114*, 129–142. [CrossRef]

33. Blanco, R. *Estudios y Propuestas de Estabilización del Cerro Las Cabras*; CIPAT-ESPOL: Guayaquil, Ecuador, 2015.

34. Grozavu, A.; Mărgărint, M.C.; Patriche, C.V. GIS applications for landslide susceptibility assessment: A case study in Iaşi county (Moldavian plateau, Romania). In *WIT Transactions on Information and Communication Technologies*; Springer: Berlin, Germany, 2010; Volume 43.

35. Lee, S.; Ryu, J.H.; Kim, I.S. Landslide susceptibility analysis and its verification using likelihood ratio, logistic regression, and artificial neural network models: Case study of Youngin, Korea. *Landslides* **2007**, *4*, 327–338. [CrossRef]

36. Morante Carballo, F.; Carrión Mero, P.; Ángel Chávez, M.; Aguilar Aguilar, M.; Briones Bitar, J. Design of the Stabilization Solutions in the General Patrimonial Cemetery of Guayaquil, Ecuador. In Proceedings of the LACCEI International Multi-Conference for Engineering, Education and Technology, Montego Bay, Jamaica, 24–26 July 2019; Latin American and Caribbean Consortium of Engineering Institutions: Boca Raton, FL, USA, 2019; Volume 2019.

37. Universo 12 Familias Saldrán del Cerro Las Cabras en Durán. Available online: http://www.eluniverso.com/noticias/2014/01/24/nota/2075171/12-familias-saldran-cerro-cabras (accessed on 15 January 2021).

38. Universo Deslaves en la Parte sur del Cerro Las Cabras. Available online: https://www.eluniverso.com/2004/02/18/0001/18/51DC33943191487EBF2C609A95D9FD23.html (accessed on 15 January 2021).

39. Durán Cerro Las Cabras. Available online: http://www.duran.gob.ec/municipio/inicio/ (accessed on 29 March 2021).

40. INEC Censo Poblacional. Available online: https://www.ecuadorencifras.gob.ec/institucional/home/ (accessed on 29 March 2021).

41. INAMHI Datos Meteorológicos e Hidrológicos. Available online: www.serviciometeorologico.gob.ec (accessed on 29 March 2021).

42. Machiels, L.; Garcés, D.; Snellings, R.; Vilema, W.; Morante, F.; Paredes, C.; Elsen, J. Zeolite occurrence and genesis in the Late-Cretaceous Cayo arc of Coastal Ecuador: Evidence for zeolite formation in cooling marine pyroclastic flow deposits. *Appl. Clay Sci.* **2014**, *87*, 108–119. [CrossRef]

43. Machiels, L.; Morante, F.; Snellings, R.; Calvo, B.; Canoira, L.; Paredes, C.; Elsen, J. Zeolite mineralogy of the Cayo formation in Guayaquil, Ecuador. *Appl. Clay Sci.* **2008**, *42*, 180–188. [CrossRef]

44. Hans, E. Thalmann. Micropaleontology of Upper Cretaceous and Paleocene in Western Ecuador. *Am. Assoc. Pet. Geol. Bull.* **1946**, *30*, 337–347.

45. Benitez, S. Évolution géodynamique de la province côtière sud-équatorienne au Crétacé supérieur—Tertiaire. *Géology Alp.* **1995**, *71*, 3–163.

46. Carrión-Mero, P.; Quiñonez-Barzola, X.; Morante-Carballo, F.; Montalván, F.J.; Herrera-Franco, G.; Plaza-Úbeda, J. Geometric Model of a Coastal Aquifer to Promote the Sustainable Use of Water. Manglaralto, Ecuador. *Water* **2021**, *13*, 923. [CrossRef]

47. Carrión-Mero, P.; Morante-Carballo, F.; Toalombo-Chimborazo, M.; Mora-Villón, D.; Briones-Bitar, J.; Berrezueta, E. Groundwater Exploration for a Susutainable Supply Plan in a Rural Community: Case Cadeate, Santa Elena, Ecuador. In Proceedings of the LACCEI International Multi-Conference for Engineering, Education and Technology, Online, 27–31 July 2020; Latin American and Caribbean Consortium of Engineering Institutions: Boca Raton, FL, USA, 2020.

48. Li, D.; Wong, L.N.Y. The Brazilian Disc Test for Rock Mechanics Applications: Review and New Insights. *Rock Mech. Rock Eng.* **2013**, *46*, 269–287. [CrossRef]

49. Andreev, G.E. A review of the Brazilian test for rock tensile strength determination. Part I: Calculation formula. *Min. Sci. Technol.* **1991**, *13*, 445–456. [CrossRef]

50. Hoek, E. Estimating Mohr-Coulomb friction and cohesion values from the Hoek-Brown failure criterion. *Int. J. Rock Mech. Min. Sci. Geomech. Abstr.* **1990**, *27*, 227–229. [CrossRef]

51. Labuz, J.F.; Zang, A. Mohr–Coulomb Failure Criterion. *Rock Mech. Rock Eng.* **2012**, *45*, 975–979. [CrossRef]

52. Deere, D.U. Technical Description of Rock Cores.pdf. *Felsmech. Ingenieurgeol.* **1963**, *I*, 18–22.

53. Palmström, A. Measurement and of rock mass jointing. In *In-Situ Characterization of Rocks—Chapter 2*; CRC Press: Boca Raton, FL, USA, 2001; pp. 1–40.

54. Carrión-Mero, P.; Solórzano, J.; Chávez, M.Á.; Blanco, R.; Morante-Carballo, F.; Aguilar, M.; Briones-Bitar, J. Evaluation of geomechanical features and stability for the recommendations and rehabilitation of the Humberto Molina Hospital, Zaruma, El Oro, Ecuador. In *Sustainable Development and Planning XI.*; WIT Press: Ashurst, UK, 2020; Volume I, pp. 455–466.

55. Chavez, M.; Guardado, R. Evaluación ingeniero-geológica del deterioro de las rocas en la provincia de Manabí, Ecuador. *Minería y Geol.* **2008**, *24*, 13.

56. Carrión-Mero, P.; Pineda-Ruiz, R.; Chávez, M.Á.; Morante-Carballo, F.; Blanco, R.; Aguilar, M.; Briones-Bitar, J. Geomechanical evaluation of the Olon cliff for stabilization pre-design of the Blanca Estrella del Mar Sanctuary, Santa Elena, Ecuador. In *Sustainable Development and Planning XI.*; WIT Press: Ashurst, UK, 2020; Volume I, pp. 467–479.

57. Suárez, J. Deslizamientos Y Estabilidad De Taludes En Zonas Tropicales. *Inst. Investig. Erosión Deslizam.* **1998**, *1*, 550.

58. López-Jimeno, C. *Manual de Estabilización y Revegetación de Taludes.*; Ediciones Graficas Árias Montano: Madrid, Spain, 1999.

59. Hoek, E.; Carter, T.G.; Diederichs, M.S. Quantification of the geological strength index chart. In Proceedings of the 47th US Rock Mechanics/Geomechanics Symposium 2013, San Francisco, CA, USA, 23–26 June 2013; Volume 3, pp. 1757–1764.

60. Hoek, E.; Brown, E.T. The Hoek–Brown failure criterion and GSI—2018 edition. *J. Rock Mech. Geotech. Eng.* **2019**, *11*, 445–463. [CrossRef]

61. Nicholson, D.T.; Hencher, S. Assesment the potential for deterioration of engineered Rock Slopes. In Proceedings of the International Symposium of Engineering and the Environment, Athens, Greece, 23–27 June 1997; pp. 911–917.

62. Ambalagán, R. Terrain Evaluation and Landslides Hazard Zonation for Environmental Regenaration and Land Use Planning in Mountainow Terrain. In Proceedings of the Sixth International Symposium on Landslide, Innsbruck, UK, 11–15 April 1992; Bell, D.H., Ed.; Wiley: Rotterdam, The Netherlands; Wiley: Christchurch, New Zealand, 1992; pp. 861–871.

63. González, A.J. Metodología y Criterios de Clasificación para Inventarios de Movimientos de Masas. In Proceedings of the Memorias I Simposio Sudamericano de Deslizamiento, Paipa, Colombia, 7–10 August 1989; Sociedad Colombiana de Geotecnia: Paipa, Colombia, 1989; pp. 677–698.

64. Carrión-Mero, P.; Aguilar-Aguilar, M.; Morante-Carballo, F.; Domínguez-Cuesta, M.J.; Sánchez-Padilla, C.; Sánchez-Zambrano, A.; Briones-Bitar, J.; Blanco-Torrens, R.; Córdova-Rizo, J.; Berrezueta, E. Surface and Underground Geomechanical Characterization of an Area Affected by Instability Phenomena in Zaruma Mining Zone (Ecuador). *Sustainability* **2021**, *13*, 3272. [CrossRef]

65. Rocscience. *Slide 5.0 Guide*; Rocscience Inc.: Toronto, ON, Canada, 2002; p. 90.

66. MIDUVI Capítulos de la NEC (Norma Ecuatoriana de la Construcción). Available online: https://www.habitatyvivienda.gob.ec/documentos-normativos-nec-norma-ecuatoriana-de-la-construccion/ (accessed on 29 March 2021).

67. Bishop, A.W. The use of the slip circle in the stability analysis of slopes. *Geotechnique* **1955**, *5*, 7–17. [CrossRef]

68. Bishop, A.W. The use of pore-pressure coefficients in practice. *Geotechnique* **1954**, *4*, 148–152. [CrossRef]

69. Melentijevic, S. Estabilidad de Taludes en Macizos Rocosos con Criterios de Rotura no Lineales y Leyes de Fluencia no Asociada. Ph.D. Thesis, E.T.S.I. Caminos, Canales y Puertos (UPM), Madrid, Spain, 2005.